Magnetic Hysteresis

Flexible Extension of Hysteresis Models for Magnetic Anisotropy

Benedikt Schauerte[1], Simon Steentjes[2], and Kay Hameyer[1]

[1]Institute of Electrical Machines, RWTH Aachen University, Aachen D52062, Germany
[2]Audi AG, Ingolstadt D85045, Germany

Received 30 Apr 2018, revised 2 Jul 2018, accepted 19 Jul 2018, published 4 Oct 2018, current version 29 Nov 2018.

Abstract—Increased demands on iron loss calculation of electrical machines require accurate models to replicate the magnetization behavior of the soft magnetic materials in any spatial direction. Two-dimensional measurement devices are developed to characterize the vector properties of the material and the power losses. These two-dimensional measurements reveal a variety of features and characteristics that cannot be reproduced by most of the conventional one-dimensional hysteresis models and their phenomenological two-dimensional extensions. This letter discusses the effect of magnetic anisotropy by using measured data obtained from a rotational power loss tester for an exemplary non-oriented electrical steel. A flexible solution that combines the entirety of crystal orientations within the material with the magneto-crystalline anisotropy is presented in this letter and discussed with respect to the general ability to recreate the observed behavior.

Index Terms—Magnetic hysteresis, anhysteretic magnetization, vector hysteresis, microparameters.

I. INTRODUCTION

The measurement and simulation of the magnetic material properties of non-oriented electrical steels have moved into the focus in the simulation of operation behavior, prototyping, and loss calculation of rotating electrical machines [Krüttgen 2017, von Pfingsten 2017]. This enhanced interest led to the development of new vector measurement devices that allow the examination of non-oriented electrical steels under rotating magnetic excitations as they occur during the operation of electrical machines. The vectorial measurement results of these devices show considerable deviations from classical one-dimensional anisotropy measurements with parallel field quantities. In addition to more precise information about the amplitudes of the magnetic field strength that are required to achieve a certain magnetization, in some cases significant phase shift between the magnetic field and flux density and the influence of the magnetic hard direction as a function of the magnetic excitation and the applied magnetic field loci originating from the magneto-crystalline anisotropy occurs [Martin 2016]. Several classic one-dimensional approaches have been adjusted, in order to extend the validity of these models to two-dimensional applications [Leite 2004, 2009, Henrotte 2006, Matsuo 2010]. In addition to these extensions of existing models, a large number of authors worked on the development of novel vector-valued hysteresis models [Matsuo 2008, Cardelli 2011, Zhu 2018], with good accuracy between measured and simulated behavior. Most of these classical hysteresis models are based on the separation of the magnetic field into lossless anhysteretic and lossy hysteretic components. Central to the replication of the magnetic anisotropy in magnetization and hysteresis models is the description of the direction-dependent anhysteretic magnetization curve [Steentjes 2017]. The anhysteretic component is often described by analytical formulas, such as the Langevin function. The adjustments performed on these models are based mainly on the addition of a second transverse set of equations, which are utilized to fill the main axis or simple analytical enhancements of the required magnetic fields that allow one to map anisotropy roughly. These simplifications lead to disadvantages regarding the recreation of the exact saturation behavior for magnetic excitations in directions between the two main axes and other phenomena that can be observed during two-dimensional measurements. Another approach as presented in Martin [2016] utilizes interpolations of measurements performed in many spatial field directions to obtain the anhysteretic relation between vector flux density $\overrightarrow{B}$ and the respective associated magnetic field strengths $\overrightarrow{H}$. This representation of the anhysteretic magnetization leads to very satisfying agreement between vector measurements and simulations, but is associated with high measurement efforts. In the following, the observed phenomenological behavior of non-oriented electrical steels under rotating excitations is presented for a commercially available M270-50A, iron-silicon steel in detail. An approach for the description of the anhysteretic material behavior based on the crystallographic texture of the material is introduced and examined in its ability to recreate the measured two-dimensional characteristics.

Corresponding author: Benedikt Schauerte (e-mail: Benedikt.Schauerte@iem.rwth-aachen.de).
Digital Object Identifier 10.1109/LMAG.2018.2874168

II. TWO-DIMENSIONAL PROPERTIES OF NON-ORIENTED ELECTRICAL STEEL

The two-dimensional magnetic measurements that will be presented in this section were performed with a four-pole rotational single-sheet tester measurement system introduced in Thul [2018]. The applied magnetic field is controlled so as to obtain circular as well as elliptical and unidirectional magnetic flux loci with adjustable amplitude and alignment in the x-y-plane. Conventionally the x-axis is assigned to the rolling direction (**RD**), the transverse direction (**TD**) to the y-axis. The magnetic flux density is measured by search coils, which are brought into drilled holes in the specimen perpendicular to RD and TD. The local magnetic field vector is obtained by H-coils that are positioned directly under the sheet [Thul 2018]. The measurements reveal a considerably anisotropy that shows the magnetic hardest behavior in the intermediate directions between the typically considered RD and TD. The impact of these hard directions increases for higher excitations

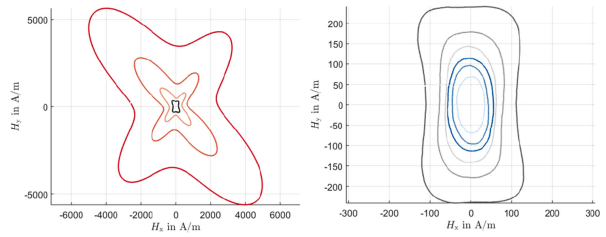

Fig. 1. Required magnetic field loci for different circular magnetic flux curves for low flux densities in 0.2 T-steps (right-hand side) and high (left-hand side) flux densities in 0.1 T-steps [Thul 2018].

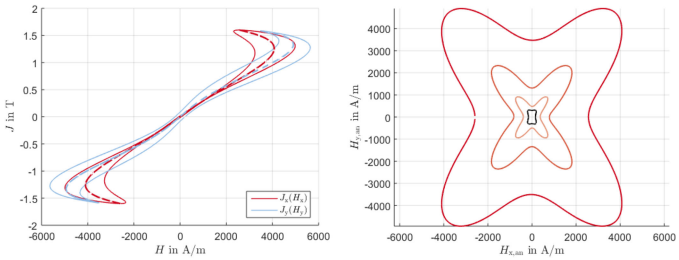

Fig. 2. Projections of measured pathways on main axes and dashed calculated anhysteretic curves (left) for rotational flux density of 1.6 T (Red line: $J_x(H_x)$. Blue line) $J_y(H_y)$) and (right) reassigned anhysteretic *H*-loci for 1.3 up to 1.6 T.

while at low magnetic flux densities the TD is the orientation with the worst magnetization behavior. Particularly at high excitations, an asymmetry regarding the required field at the magnetic hard directions occurs, which depends on the rotational direction of the applied field. The measured pathways can be regarded with their projections on the main axes. The anhysteretic curves can be approximated by averaging the magnetic field with respect to the polarization *J*. Assigning the anhysteretic magnetic fields to the affiliated polarizations, taking into account the temporal order of the vector components, the anhysteretic magnetic field loci for rotational polarizations can be obtained.

The anhysteretic field loci, depicted in Fig. 2, lack the asymmetries that can be observed for the hysteretic magnetic field components in Fig. 1. Next to the anisotropic field requirements, a closer examination of the obtained anhysteretic vectors reveals a considerable phase shift between the circulating flux density and the required magnetic field orientations of the polarization and strongly depends on the magnetic excitation, having a peak-to-peak value of almost 40°, as depicted in Fig. 3. This phase difference varies with the spatial low magnetizations, where a more colinear behavior could be expected as the material is still in its linear region. The phase difference decreases at regions of higher magnetizations until there is a change of the phase differences sign. While for lower magnetizations, the two easy directions of magnetization occur to be the most remarkable influences, at higher excitations the four magnetic hard directions are clearly visible as peaks along the curve for 1.6 T. Regarding the information of Figs. 1 and 3, a connection between the respective magnetic hardest directions and the peaks of the phase difference between applied magnetic field and resulting flux density can be denoted. Although the measurements have not yet been reduced by their respective hysteretic components, the need for an anhysteretic description that is able to replicate the observed characteristics can be pointed out. As a collinear description of the vector behavior is always connected with considerably error, even though the respective curves can be replicated accurately, an approach that aims for a higher agreement with the vectorial material behavior is determined to take into account the observed phase shift. This mentioned phase shift includes the time dependence that is lost at the alone standing typical pictorial representations of the obtained $J_x - J_y$ respective $H_x - H_y$-loci, as depicted in Fig. 1.

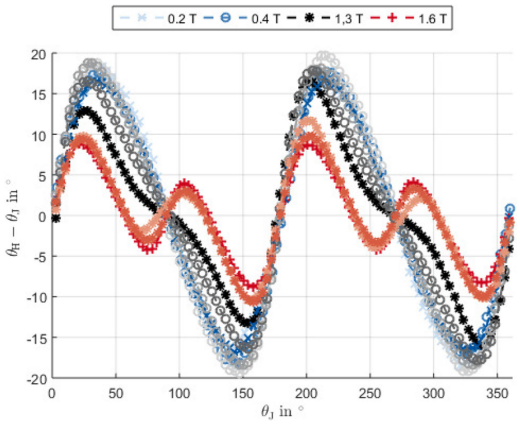

Fig. 3. Phase difference between anhysteretic $\vec{H}$ and $\vec{B}$ vectors at different circular polarizations.

III. TEXTURE AND ORIENTATION DISTRIBUTION FUNCTION

Non-oriented electrical steel is composed out of a multitude of grains in which the iron crystals are oriented collinearly. The misalignment between the respective crystal orientations and the applied field is decisive for the magnetization behavior of the material and, thus, for the global measurable magnetic anisotropy. Commonly, the magnetizability of a single iron grain is distinct in magnetic hard, medium, and easy directions. This characteristic is based on the arrangement of the atoms within the crystal grid and the interaction of their respective magnetic moments. The energy that an iron crystal has to supply to turn its magnetic moment into a specific direction described in azimuthal angles can be calculated by [Bertotti 1998]

$$W_{An} = K_0 + K_1\left(\alpha_x^2\alpha_y^2 + \alpha_y^2\alpha_z^2 + \alpha_z^2\alpha_x^2\right) \tag{1}$$

with the anisotropy coefficients K_0 set to 0 and $K_1 = 45\ \mathrm{kJ/m^3}$ [Blügel 1999].

A three-dimensional energy surface is obtained that can be deformed by the application of an external magnetic field, which makes it easier for the crystal to align its magnetic moment collinearly to the field direction. This energy contribution of the applied field is the Zeeman energy and can be described by the applied field vector $\vec{H}$ and the respective orientation of the magnetic moment [Daniel 2015]

$$W(\vec{m}) = W_{An}(\vec{m}) - \vec{H}\cdot\vec{m}. \tag{2}$$

As the direction of the magnetization has a remarkable influence on the magnetic behavior of a single crystal, the global description of the entirety of crystals is of high importance for the analysis of the materials' anisotropic behavior. To describe all crystal positions of the grains inside the material (the texture) to a mutual reference system, a mathematical description of the crystals orientations has to be introduced. This purpose is fulfilled by three Euler angles that give a unique description of each of the crystal orientations with respect

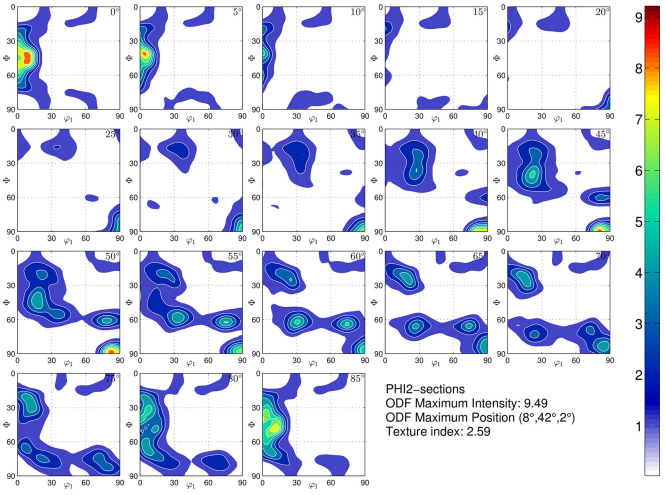

Fig. 4. Graphical representation of ODF of a typical non-oriented electrical steel.

to the global common rolling-transverse-normal direction reference system by three angles [Kestens 2008].

The different crystal orientations can be weighted by their respective ratio of the total volume of the examined material, in order to obtain an orienation distribution function (**ODF**) of the material texture. The ODF $p(g)$ provides the volume fraction of the crystals for the given orientation g, described by three Euler angles. As the graphical presentation of three-dimensional functions is linked with several difficulties, the ODF is presented by several cuts along the φ_2-axis, as depicted in Fig. 4. At each cut along the φ_2-axis the volume fraction of each crystal-orientation is pictured by the respective color with respect to the other two assigned angles.

IV. MODEL APPROACH

The objective is to achieve a two-dimensional description of the anhysteretic curve that matches with the previously described measured behavior for rotational as unidirectional excitations. Thus, it is recommendable to rely on the microstructural characteristics, which cause the specific effects that are to be recreated.

Combining the quantified information about the different orientations of the iron crystals within the examined material with the anisotropy energy, a semi-physical representation of the materials anisotropic behavior can be obtained. For each set of angles g that occurs in the ODF, the anisotropic energy surface is calculated in the corresponding orientation with respect to the global reference system. The rotated energy crystals are superposed and weighted by the value of their respective volume ratio p(g) described by the ODF. By this means, a representative energy crystal describing the anisotropy energy $W_{\mathrm{An,rep}}$ of the examined material can be obtained. The representative energy crystal for the actual considered M270-50A material calculated by this method is depicted in Fig. 5. The distance between the actual point on the energy surface and the origin of the coordinate system denotes the amount of energy that has to be made up by the crystal to allow the orientation of the magnetic moment in the respective direction of m. The representative energy crystal can also be understood as a visualization of the information included in the ODF.

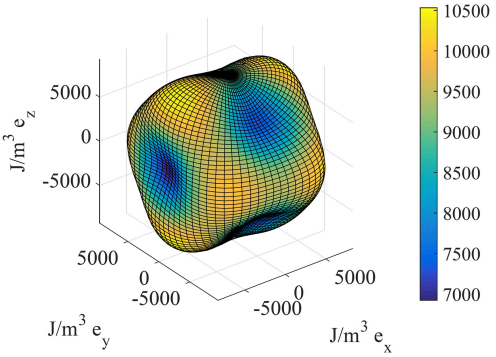

Fig. 5. Calculated averaged energy-crystal based on ODF and magneto-crystalline anisotropy energy.

The shape of the energy surface reveals a distinctive easy direction in the RD. A magnetic harder behavior for the TD and particularly the magnetic hardest directions between the main axes are visible. In general, the material appears to have magnetic properties that reveal similarities with Goss-textured grain-oriented materials as described in Cardelli [2017], even though they are not so distinctive. In addition to these qualitative statements about the anisotropic behavior of the material, the representation of the anisotropy energy of the material can be utilized in order to obtain quantitative results. In combination with the Zeeman energy, which describes the influence of an applied magnetic field, the representative energy crystal can be deformed as

$$W_{\mathrm{rep}}(\vec{m}) = W_{An,\,\mathrm{rep}}(\vec{m}) - \mu_0 \vec{H} \cdot \vec{m}. \tag{3}$$

Combining this deformed energy surface with the Boltzmann distribution, a probability f that a certain energy state W_{rep} occurs can be derived [Daniel 2014]

$$f(\vec{m}) = \frac{\exp(-W_{\mathrm{rep}}(\vec{m}))}{\int \exp(-W_{\mathrm{rep}}(\vec{m}) \cdot d\vec{m})}. \tag{4}$$

Calculating this probability f for each orientation of m on the energy surface, the magnetization in RD and TD can be determined as a function of the applied field H by an integration over the unit sphere and projecting the respective magnetic moments by their angle to the x-axis and y-axis

$$M_x(\vec{H}) = M_S \cdot \int f(\vec{m}) \cdot \cos(\alpha_x) \cdot d\vec{m} \tag{5}$$

$$M_y(\vec{H}) = M_S \cdot \int f(\vec{m}) \cdot \cos(\alpha_y) \cdot d\vec{m}. \tag{6}$$

By this means, an energy-based formulation for the description of anhysteretic vector magnetization that considers the material's microparameters is obtained. Further adjustments such as temperature dependence or mechanical stress could also be applied to the energy surface of the representative energy crystal by additional three-dimensional energetic descriptions. In the original form, the texture-based description of the anhysteretic magnetization provides a calculated vector-polarization $\vec{H}$ as a function of the applied magnetic field vector $\vec{J}$. The model can be inverted by numerical methods, yielding the vector magnetic field solution causing a predetermined magnetic flux density. The resulting magnetic field loci for circular polarizations according to the measurements were identified. The results show

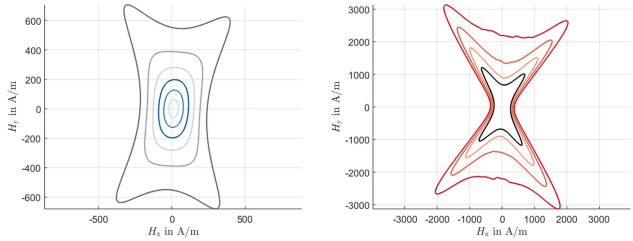

Fig. 6. Simulated anhysteretic magnetic field loci for low (left-hand side) and high (right-hand side) circular polarizations.

a qualitatively similar behavior to the measurements result, as shown in Fig. 6.

V. RESULTS

Starting with elliptical curves at low polarizations, the calculated shapes change into more rectangular curves. Over the entire range, the TD direction reveals higher required field strengths. For higher polarizations, entering the saturation area, the impact of the magnetic hard directions at an angle of approximately 55° misalignment to the RD is replicated with accordance to the measurements. The simulated field loci are slightly twisted in comparison to the measurements. An effect that occurs due to the discretization of the representative energy surface. As the measurements revealed considerable phase differences between the applied magnetic field vectors $\vec{H}$ and the resulting polarization $\vec{J}$, the ability of the description to replicate this behavior is crucial for the evaluation of the models' ability to recreate the anhysteretic components of the magnetic field quantities. Again, the measured pathways are recreated with qualitatively good accordance. The characteristic curves at the different excitations are recreated. Starting from the sinusoidal appearing curves for low polarizations with a stronger slope at the ascending branch that is recreated by the model, the transition to the more complex pathways with additional amplitudes originating from the higher required fields at the magnetic harder directions is imitated. Despite the similarity regarding the curves of simulation and measured phase difference, the results show deviations from the measurements in terms of amplitudes and offset. In general, the representative crystal appears to recreate the measured behavior satisfactory but to sensitive regarding the applied field and the reaction on its deformation. Further examinations considering the linkage between different grains and their interaction could also lead to quantitative correct results. Thus, it can be denoted that the model is able to represent the magnetic anhysteretic behavior in terms of anisotropy, two-dimensionality, and phase difference.

VI. CONCLUSION

In this letter, the requirements for an appropriate vectorial formulation of the anhysteretic magnetization are defined and presented exemplarily for a non-oriented electrical steel with strong anisotropy. Based on the materials texture, a semiphysical approach for the calculation of the anhysteretic magnetization is presented, which can be used in a variety of classical hysteresis models, which are based on the separation into hysteretic and anhysteretic components. As the proposed description can be inverted, it can be utilized in direct and inverted vector hysteresis models. While the qualitatively behavior is recreated with good accuracy, further adaptations are required to achieve quantitative satisfying results.

ACKNOWLEDGMENT

This work was supported in part by the research project group project "SP-2013 - The utilization of residual stresses induced by metal forming" funded by the Deutsche Forschungsgesellschaft (DFG) HA 4395/22-1 as DFG 255713208 and in part by the research group project "FOR 1897 Low-Loss Electrical Steel for Energy-Efficient Electrical Drives".

REFERENCES

Bertotti G (1998), *Hysteresis in Magnetism: For Physicists, Materials Scientists, and Engineers*. New York, NY, USA: Academic.

Blügel S (1999), *Magnetische Anisotropie und Magnetostriktion (Materie und Material, 2)*. Jülich, Germany: Schriften des FZ-Jülich.

Cardelli E (2011), "A general hysteresis operator for the modeling of vector fields," *IEEE Trans. Magn.*, vol. 47, pp. 2056–2067, doi: 10.1109/TMAG.2011.2126589.

Cardelli E, Faba A, Laudani A, Pompei M, Antonio S Q, Fulginei F R, Salvini A (2017), "A challenging hysteresis operator for the simulation of Goss-textured magnetic materials," *J. Magn. Magn. Mater.*, vol. 432, pp. 14–23, doi: 10.1016/j.jmmm.2017.01.068.

Daniel L, Hubert O, Rekik M (2015), "A simplified 3-D constitutive law for magnetomechanical behavior," *IEEE Trans. Magn.*, vol. 51, 7300704, doi: 10.1109/TMAG.2014.2361643.

Daniel L, Rekik M, Hubert O (2014), "A multiscale model for magneto-elastic behaviour including hysteresis effects," *Arch. Appl. Mech.*, vol. 84, pp. 1307–1323, doi: 10.1007/s00419-014-0863-9.

Henrotte F, Hameyer K (2006), "A dynamical vector hysteresis model based on an energy approach," *IEEE Trans. Magn.*, vol. 42, pp. 899–902, doi: 10.1109/TMAG.2006.872473.

Kestens L, Jacobs S (2008), "Texture control during the manufacturing of nonoriented electrical steels," *Texture, Stress, Microstruct.*, vol. 2008, 173083, doi: 10.1155/2008/173083.

Krüttgen C, Steentjes S, Glehn G, Hameyer K (2017), "Parametric homogenized model for inclusion of eddy currents and hysteresis in 2-D finite element simulation of electrical machines," *IEEE Trans. Magn.*, vol. 53, 7001004, doi: 10.1109/TMAG.2017.2660460.

Leite J V, Benabou A, Sadowski N, da Luz M V F (2009), "Finite element three-phase transformer modeling taking into account a vector hysteresis model," *IEEE Trans. Magn.*, vol. 45, pp. 1716–1719, doi: 10.1109/TMAG.2009.2012794.

Leite J V, Sadowski N, Kuo-Peng P, Batistela N J, Bastos J P A, de Espindola A A (2004), "Inverse Jiles-Atherton vector hysteresis model," *IEEE Trans. Magn.*, vol. 40, pp. 1769–1775, doi: 10.1109/TMAG.2004.830998.

Martin F, Singh D, Rasilo P, Belahcen A, Arkkio A (2016), "Model of magnetic anisotropy of non-oriented steel sheets for finite-element method," *IEEE Trans. Magn.*, vol. 52, 7002704, doi: 10.1109/TMAG.2015.2488100.

Matsuo T (2010), "Anisotropic vector hysteresis model using an isotropic vector play model," *IEEE Trans. Magn.*, vol. 46, pp. 3041–3044, doi: 10.1109/TMAG.2010.2043822.

Matsuo T (2008), "Rotational saturation properties of isotropic vector hysteresis models using vectorized stop and play hysterons," *IEEE Trans. Magn.*, vol. 44, pp. 3185–3188, doi: 10.1109/TMAG.2008.2001656.

von Pfingsten G, Steentjes S, Hameyer K (2017), "Operating point resolved loss calculation approach in saturated induction machines," *IEEE Trans. Ind. Electron.*, vol. 64, pp. 2538–2546, doi: 10.1109/TIE.2016.2597761.

Steentjes S, Henrotte F, Hameyer K (2017), "Energy-based ferromagnetic material model with magnetic anisotropy," *J. Magn. Magn. Mater.*, vol. 425, pp. 20–24, doi: 10.1016/j.jmmm.2016.10.085.

Thul A, Steentjes S, Schauerte B, Klimczyk P, Denke P, Hameyer K (2018), "Rotating magnetizations in electrical machines: Measurements and modeling," *AIP Adv.*, vol. 8, 056815, doi: 10.1063/1.5007751.

Zhu L, Park J, Koh C-S (2018), "A dynamic hysteresis model based on vector-play model for iron loss calculation taking the rotating magnetic fields into account," *IEEE Trans. Magn.*, vol. 54, 7300404, doi: 10.1109/TMAG.2017.2748961.